

Electrochemical and Catalytic Properties of oxo-ruthenate(VI) in Aqueous Alkaline Medium

Abdel Ghany F. Shoair¹ Mai M. A. H. Shanab², Mohamed H. H. Mahmoud³

¹ Department of Science and Technology, University College - Ranyah, Taif University, Saudi Arabia

² Department of Chemistry, Sciences & Humanities Studies College, Hawtat Bani Tamim, Prince Sattam Bin Abdul-Aziz University, Al-Kharj, Saudi Arabia

³ Department of Chemistry, College of Science, Taif University, P.O. Box 11099, Taif, 21944, Saudi Arabia

*E-mail: afshaair@tu.edu.sa

Received: 4 January 2021 / Accepted: 6 March 2021 / Published: 31 March 2021

The complex $K_2[Ru^{(III)}Cl_5(H_2O)]$ has been prepared and characterized by different spectroscopic techniques (IR and UV-VIS). The electrochemical properties of this complex were investigated at different pH's using Robinson buffer solutions. The cyclic voltammograms exhibited three redox different oxidation and potential peaks due to generation of Ru(III), Ru(IV), Ru(V) and Ru(VI) ions. The catalytic activity of $K_2[Ru^{(III)}Cl_5(H_2O)]$ towards the hydration of some aromatic and three heterocyclic nitriles to their corresponding amides was investigated with excess of three co-oxidants $K_2S_2O_8$, NaOCl and $KBrO_3$. A number of factors have been investigated and the best yields were obtained with $K_2S_2O_8$ as a co-oxidant in a 1.0 M KOH at 80 °C. Both spectroscopic and electrochemical techniques were used to establish the nature of active species in this catalytic reaction and the active catalyst was found to be $K_2[Ru^{(VI)}O_3(OH)_2]$, as well as to explain the possible reaction mechanism. The suggested mechanism included the coordination of nitrile to ruthenium center followed by liberation of the corresponding amide and the active complex again.

Keywords: ruthenium, catalytic hydration, co-oxidant

1. INTRODUCTION

The electronic distribution of ruthenium metal $[Kr]5s^14d^7$, made it possesses a large number of oxidation states among the other transition elements from -2 in $[Ru(CO)_5]$ to +8 in $[RuO_4]$. Additionally, the high electron transfer capacity that made it able to stabilize high oxidation states such as oxo-metal complexes which are a good catalysts for many catalytic oxidation processes [1-27]. The amide is one of the most important organic compounds and is present in many of natural products, however, although many methods were reported, these methods suffer from harsh reaction condition

[28]. A number of (hetero)aryl and alkyl nitriles were converted to amides with NaOH as the catalyst in $\text{NH}_3 \cdot \text{H}_2\text{O}$ –DMSO mixture [29]. Other transition metals were used for hydration of nitrile to amide, hydroxyapatite (HAP)-supported on silver NPs (AgHAP) stoichiometrically hydrated benzonitrile to benzamide at 140 °C in water [30]. The osmium complex $[\text{Os}(\eta^6\text{-}p\text{-cymene})(\text{OH})\text{IPr}]\text{OTf}$ (IPr = 1,3-bis(2,6-diisopropylphenyl)imidazolylidene; OTf = CF_3SO_3) has proved to be an efficient catalyst for hydration of a wide range of aromatic and aliphatic nitriles to their corresponding amides at 120 °C [31]. $\text{RuCl}_3 \cdot n\text{H}_2\text{O}$ and six equivalent of PTA (PTA=1,3,5-triaza-7phosphaadamantane) converted benzonitrile to benzamide at 100 °C for in aqueous-phase in 93% yield [32]. The new Ru-dmsO complex with bidentate pyridylpyrazole ligands, $[\text{Ru}^{\text{II}}\text{Cl}_2(\text{pypz-Me})(\text{dmsO})_2]$ was synthesized and fully characterized. The complex was found to be active toward catalytic hydration benzonitrile to amide in the homogeneous phase, with moderate to high conversion values [33]. The single X-ray crystal structure of the ammonium salt of $[\text{Ru}^{\text{III}}\text{Cl}_5(\text{H}_2\text{O})]^{2-}$ anion was reported [34] and therefore we prepared the corresponding potassium salt $\text{K}_2[\text{Ru}^{\text{III}}\text{Cl}_5(\text{H}_2\text{O})]$ and studied the catalytic activity of this complex towards a number of organic compounds under ultrasonic conditions [35]. This prompted us for further studies on the electro and the catalytic properties this complex towards conversion of some aromatic and heterocyclic nitriles to their corresponding amides using a better improved protocol than that has been used in our early published work [35]. The nature of active species was investigated by spectroscopic and electrochemical techniques, and a plausible mechanism was suggested.

2. EXPERIMENTAL METHODS

2.1. Materials

Ruthenium trichloride trihydrate and benzonitrile, *p*-hydroxybenzonitrile, *p*-aminobenzonitrile, *p*-methylbenzonitrile, *p*-trifluorobenzonitrile, *p*-formylbenzonitrile, *p*-nitrobenzonitrile, 4-cyanopyridine, 2-furonitrile and 2-thiophenecarbonitrile, $\text{K}_2\text{S}_2\text{O}_8$ and NaOCl (5%) were obtained from Sigma and were used without further purification. Robinson Buffer solution of different pH's and stock solutions of 1 mM of $\text{K}_2[\text{Ru}^{\text{III}}\text{Cl}_5(\text{H}_2\text{O})]$ were prepared in deionized water and stored at 4 °C. All supporting electrolyte solutions were prepared using analytical grade reagents and purified water.

2.2. Physical measurements

Voltammetric experiments were carried out using a three-electrode electrochemical cell (a glassy carbon (GCE) ($d = 1.5$ mm) working electrode, a Pt wire counter electrode, and Ag/AgCl (3 M KCl) as reference electrode connected with a computerized voltammetric analyzer CHI610C. The electrochemical analyzer controlled by CHI Version 9.09 software (CH Instruments, USA) and the data (E_{p1a} , E_{p2a} and E_{p3a} are the anodic, while E_{p1c} , E_{p2c} and E_{p3c} are the cathodic cyclic voltammetric peaks potentials respectively) are reported *versus* the redox couple of Fe(II) of ferrocene i.e. $\text{FcH}/\text{FcH}^+(\text{V})$. All measurements employed Robinson buffer of different pH's at a constant temperature of 25 ± 0.5 °C as a supporting electrolyte. Infrared spectra were recorded on Mattson 5000

FT-IR and electronic spectra were recorded on UV-visible vision software V. 3. The ^1H NMR spectra were recorded on a Bruker WP 400 MHz using d_6 -dmsO as a solvent containing TMS as the internal standard.

2.3. Synthesis of $\text{K}_2[\text{Ru}^{(\text{III})}\text{Cl}_5(\text{H}_2\text{O})]$

The complex was prepared according to literature procedure [36] with some modification.

Ruthenium chloride trihydrate, $\text{RuCl}_3 \cdot 3\text{H}_2\text{O}$ (131 mg, 0.5 mM) was added to 50 mL of 12 N concentrated HCl and refluxed for 5 hrs. Potassium chloride (113 mg, 15 mM) was introduced into this hot solution producing an immediate black precipitate. The precipitate was collected by filtration, dried and dissolved in 100 mL of 6 N HCl. The filtrate was evaporated to its half volume and cooled. Upon cooling a deep red crystals were formed, filtered, washed with 95% ethanol, ether and air dried. The infrared spectrum of $\text{K}_2[\text{Ru}^{(\text{III})}\text{Cl}_5(\text{H}_2\text{O})]$ gave two bands at 400 cm^{-1} and 280 cm^{-1} and the electronic spectrum in water gave two bands (λ_{max}) at 298 nm and 396 nm.

2.4 . Synthesis of $\text{K}_2[\text{Ru}^{(\text{VI})}\text{O}_3(\text{OH})_2]$

To a 25-ml quick fit flask, 10 mL of 1.0 M KOH, $\text{K}_2[\text{Ru}^{(\text{III})}\text{Cl}_5(\text{H}_2\text{O})]$ (37.5 mg, 0.1 mM) were added respectively with constant stirring for 10 minutes. The co-oxidant, $\text{K}_2\text{S}_2\text{O}_8$ (81 mg, 0.3 mM) was added with continual stirring until the appearance of a red-orange color. The solution was diluted with 1.0 M KOH and the UV-vis spectrum of the diluted solution was recorded. The UV-vis spectrum (nm) gave two bands at 462 nm and 365 nm.

2.5. General procedure for catalytic hydration of nitriles

To a 25 mL of a quick fit flask, 10 mL of 1.0 M KOH, $\text{K}_2\text{S}_2\text{O}_8$ (810 mg, 3 mM) and $\text{K}_2[\text{Ru}^{(\text{III})}\text{Cl}_5(\text{H}_2\text{O})]$ (7.5 mg, 0.02 mM) were added. The mixture was stirred for 30 minutes until the appearance of a red-orange solution. The nitrile (2 mM) was then added and the reaction mixture was refluxed at $80\text{ }^\circ\text{C}$ in a thermostated water-bath for 4 hours during which the red-orange color gradually disappeared. The produced amide was then extracted by ethylacetate and the extracts were dried over anhydrous Na_2SO_4 , evaporated and identified by IR, melting point and ^1H NMR where appropriate.

Benzamide: Colorless plates (230 mg, 95 % yield).

m.p: $126\text{--}127\text{ }^\circ\text{C}$ (lit. [35b], $125\text{--}128\text{ }^\circ\text{C}$).

IR (KBr): $\nu(\text{CO})$; 1649, 1660, $\nu(\text{NH}_2)$; 3124, 3340, 3400 cm^{-1}

^1H NMR (400 MHz, CDCl_3): δ (ppm); 7.5 (bs, 1H), 7.62-7.27 (m, 2H), 7.31 (tt, $J = 1.5, 7.3\text{ Hz}$, 1H), 7.55-7.7 (m, 2H), 7.8 (bs, 1H).

p-Hydroxybenzamide: White powder, (260.5 mg, 95 % yield).

M.p.: $156\text{--}158\text{ }^\circ\text{C}$ (lit. [35b], $148\text{ }^\circ\text{C}$).

IR (KBr): $\nu(\text{CO})$; 1659, 1655, $\nu(\text{NH}_2)$; 3200, 3310, 3390 cm^{-1}

^1H NMR (d_6 -dmsO, 400 MHz) δ (ppm); 6.7 (d, $J = 8.7$ Hz, 2H), 7.3 (bs, 1H), 7.58-7.7 (m, 3H), 9.64 (s, 1H).

***p*-Aminobenzamide:** Light yellow blocks (256 mg, 94 % yield).

m.p.: 176.3–180.9 °C (lit. [35b], 180 - 183 °C).

IR (KBr): $\nu(\text{CO})$; 1651, 1670, $\nu(\text{NH}_2)$; 3144, 3350, 3380 cm^{-1}

^1H NMR (400 MHz, d_6 -dmsO): δ (ppm); 5.59 (s, 2H), 6.53 (d, $J = 8.6$ Hz, 2H), 6.86 (bs, 1H), 7.53 (bs, 1H),

***p*-Methylbenzamide:** Colorless plates, (254 mg, 94 % yield).

m.p. 157-160 °C (lit. [35b], 159 - 160 °C).

IR (KBr): $\nu(\text{CO})$; 1646, 1666, $\nu(\text{NH}_2)$; 3154, 3370, 3400 cm^{-1}

^1H NMR (400 MHz, d_6 -dmsO): δ (ppm); 2.44 (s, 3H), 7.32–7.50 (m, 3H), 7.65–7.70 (m, 2H), 7.80 (bs, 1H).

***p*-(trifluoromethyl)benzamide:** White powder, (310 mg, 82 % yield).

M.p.: 182–185 °C (lit. [35b], 184-186 °C).

IR (KBr): $\nu(\text{CO})$; 1647, 1675, $\nu(\text{NH}_2)$; 3210, 3320, 3390 cm^{-1}

^1H NMR (400 MHz, d_6 -dmsO): δ (ppm); 7.2 - 7.9 (m, 2H), 8.30–8.40 (m, 2H).

4-Formylbenzamide: White solid (251 mg, 84% yield).

m.p.: 178–183 °C (lit. [35b], 182 °C).

IR (KBr): $\nu(\text{CO})$; 1640, 1672, $\nu(\text{NH}_2)$; 3134, 3339, 3389 cm^{-1}

^1H NMR (400 MHz, d_6 -dmsO): δ (ppm); 10.2 (bs, 1H), 8.19 (bs, 1H), 7.87 (d, $J = 7.85$ Hz, 2H), 7.89 (d, $J = 8.0$ Hz, 2H), 7.52 (bs, 1H).

***p*-Nitrobenzamide:** Colorless needles (282 mg, 85 % yield).

m.p. 196 - 200.0 °C (lit. [35b], 200 °C).

IR (KBr): $\nu(\text{CO})$; 1659, 1674, $\nu(\text{NH}_2)$; 3130, 3330, 3400 cm^{-1}

^1H NMR (400 MHz, d_6 -dmsO): δ (ppm); 8.2 - 8.3 (m, 2H), 8.40–8.50 (m, 2H).

Furan-2-carboxamide: White solid (211 mg, 95% yield).

m.p.: 141-142 °C (lit. [35b], 143 °C).

IR (KBr): $\nu(\text{CO})$; 1640, 1670, $\nu(\text{NH}_2)$; 3140, 3360, 3400 cm^{-1}

^1H NMR (400 MHz, d_6 -dmsO): δ (ppm); 7.73 (t, $J = 0.7$ Hz, 1H), 7.60 (bs, 1H), 7.51 (bs, 1H), 7.24 (d, $J = 3.4$ Hz, 1H), 6.72 (q, $J = 1.7$ Hz, 1H).

Thiophene-2-carboxamide: White solid (234 mg, 92 % yield).

m.p.: 177-179 °C (lit. [35b], 180 °C).

IR (KBr): $\nu(\text{CO})$; 1654, 1672, $\nu(\text{NH}_2)$; 3144, 3350, 3400 cm^{-1}

^1H NMR (400 MHz, d_6 -dmsO): δ (ppm); 7.85 (bs, 1H), 7.64 (s, 2H), 7.47 (bs, 1H), 7.35 (t, $J = 3.9$ Hz, 1H).

Isonicotinamide: White solid (229.6 mg, 94 % yield).

m.p.: 151.1-153 °C (lit. [35b], 154 °C).

IR (KBr): $\nu(\text{CO})$; 1660, 1670, $\nu(\text{NH}_2)$; 3134, 3320, 3388 cm^{-1}

^1H NMR (400 MHz, d_6 -dmsO): δ (ppm); 8.64 (dd, $J = 4.3$ and 1.5 Hz, 2H), 7.68 (dd, $J = 4.3$ and 1.6 Hz, 2H).

3. RESULTS AND DISCUSSION

3.1. Synthesis of $K_2[Ru^{(III)}Cl_5(H_2O)]$ and $K_2[Ru^{(VI)}O_3(OH)_2]$

The procedure of Buckley [36] was used with some modification for the preparation of $K_2[Ru^{(III)}Cl_5(H_2O)]$. The infrared spectrum of $K_2[Ru^{(III)}Cl_5(H_2O)]$ displayed two bands at 400 cm^{-1} and 280 cm^{-1} Figure 1. The UV-vis spectra of $K_2[Ru^{(III)}Cl_5(H_2O)]$ and the *in situ* generated, $K_2[Ru^{(VI)}O_3(OH)_2]$ are shown in Figure 2.

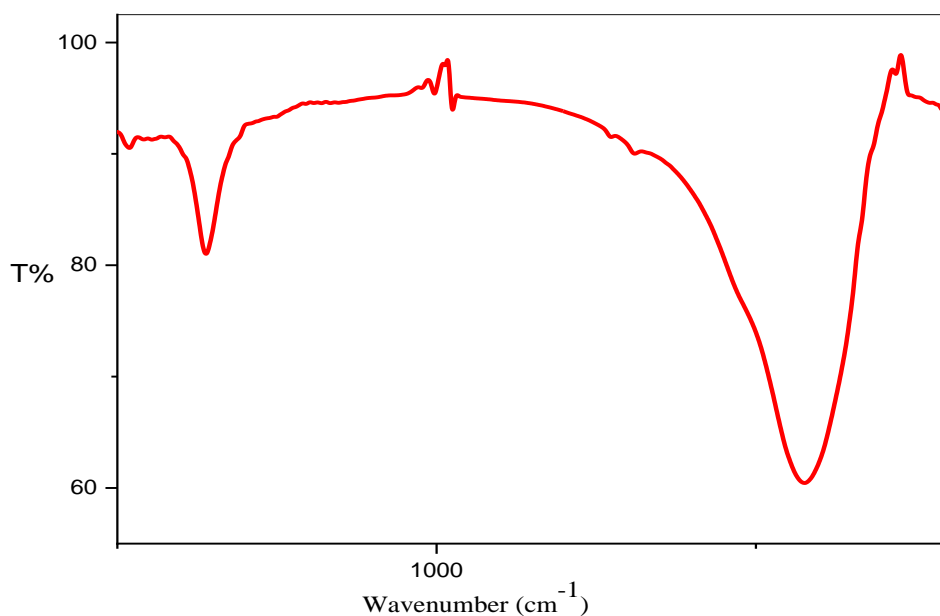


Figure 1. The infrared spectrum of $K_2[Ru^{(III)}Cl_5(H_2O)]$

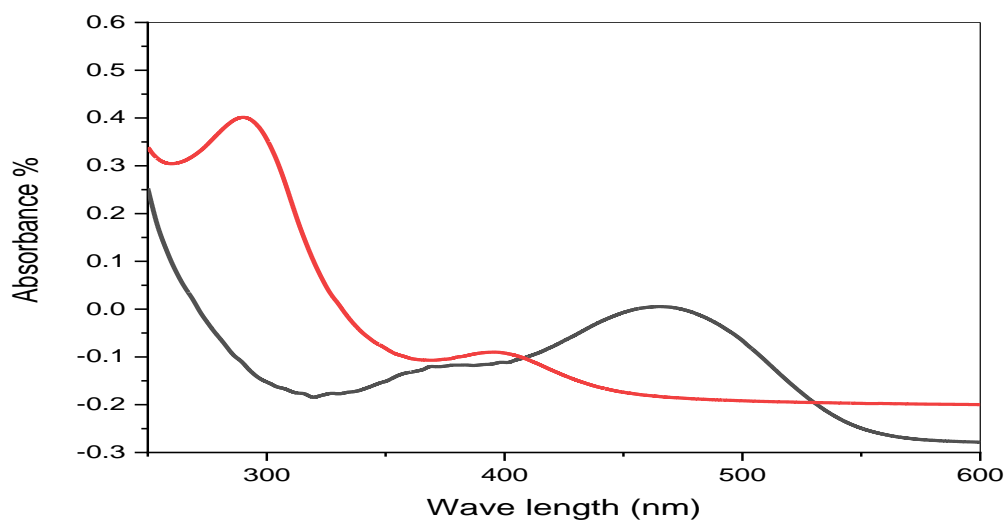
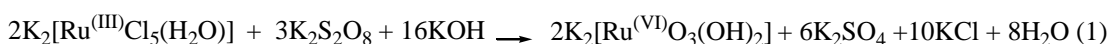


Figure 2. The UV-vis spectra of $K_2[Ru^{(III)}Cl_5(H_2O)]$ (red line) and $K_2[Ru^{(VI)}O_3(OH)_2]$ (black line) complexes

The UV-vis spectrum of $K_2[Ru^{(III)}Cl_5(H_2O)]$ in water gave two bands at 396 and 298 nm, attributable to d-d transition and n- σ transitions respectively, these bands are similar to those reported by Fine [37]. The use of oxo-transfer reagents were used for conversion of Ru^{III} complexes to Ru^{VI} complexes, the complex $trans-[Ru^{III}(Cl)_2(14-TMC)]^+$ was oxidized to $trans-[Ru^{VI}(O)_2(14-TMC)]^{2+}$ in boiling water by an aqueous 30% H_2O_2 [38-39], therefore we prepared $K_2[Ru^{(VI)}O_3(OH)_2]$ by oxidation of $K_2[Ru^{(III)}Cl_5(H_2O)]$ by an excess of $K_2S_2O_8$ in an aqueous 1.0 M KOH at room temperature equation (1). The UV-vis spectrum of $K_2[Ru^{(VI)}O_3(OH)_2]$ gave bands at 462 nm and 365 nm, these bands are close to those reported by Shoair [40] and Griffith [41] also are in agreement with the classical work reported by Connik and Hurley [42].



3.2. Electrochemistry of $K_2[Ru^{(III)}Cl_5(H_2O)]$ in Alkaline Solution.

The *in situ* generation of $K_2[Ru^{(VI)}O_3(OH)_2]$ from $K_2[Ru^{(III)}(C_2O_4)_3]$ was reported [40]. Though we investigated the cyclic voltammetry of $K_2[RuCl_5^{(III)}(H_2O)]$ at pH 12, but there were some uncertainties in current-potential profile [35]. This prompted us to investigate in details the electrochemical properties of this complex by cyclic voltammetry (CV) at a platinum electrode in electrolytes with different pH's (pH from 10 to 14). This will be useful for establishment of the nature of the oxo-ruthenium species electrochemically formed and suggestion of a plausible mechanism. The data are presented in Table 1 and the cyclic voltammograms are shown in Figure 3. At pH = 10, Figure 3(A), the cyclic voltammogram displayed three anodic (1a, 2a and 3a) and three cathodic (1c, 2c and 3c) peaks. These are probably due to oxidation of the complex to higher oxidation states than +3. The three oxidation peaks were occurred as follows: peak 1a at $E_{p1a} = -0.074$ mV, peak 2a, $E_{p2a} = 0.697$ mV and peak 3a, $E_{p3a} = 0.886$ mV. These peaks are attributable to transition of Ru(III) to Ru(IV), Ru(IV) to Ru(V) and Ru(V) to Ru(VI) respectively. However, $[Ru^{(V)}O_4]$ is unstable and formed as intermediate during the formation of the well-known ruthenate $[Ru^{(VI)}O_3(OH)_2]^{2-}$ [43].

On the negative-going scan, the corresponding reduction peaks are peak 1c at $E_{p1c} = -0.393$ mV, peak 2c, at $E_{p2c} = 0.320$ mV and peak 3c, at $E_{p3c} = 0.757$ mV, these peaks are assigned to the reduction of Ru(IV) to Ru(III), Ru(V) to Ru(IV) and Ru(VI) to Ru(V) respectively. It is observed that the intensity of the wave due to Ru(III)/Ru(IV) is lower than that of Ru(IV)/Ru(V) which in turn is lower than that of Ru(V)/Ru(IV), this is probably due to slow electron transfer from the solution to the electrode surface. Equations (2, 3 and 4) illustrate the expected species that can be formed:

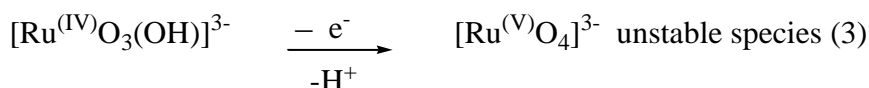
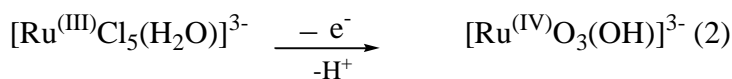
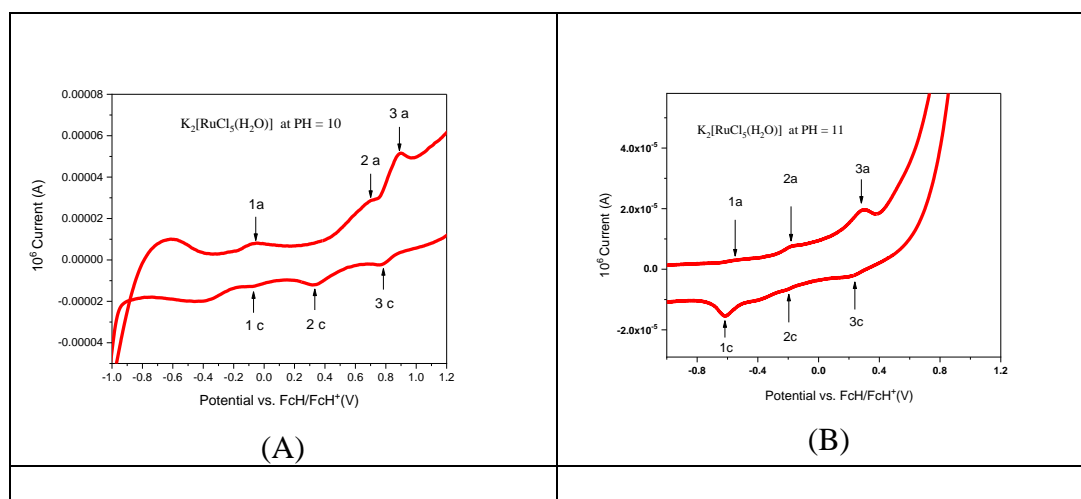


Table 1. Electrochemical data of $\text{K}_2[\text{Ru}^{\text{III}}\text{Cl}_5(\text{H}_2\text{O})]$ at different pH's (potential in mV vs. FcH/FcH^+)

Redox couple	$\text{Ru}^{\text{III}}/\text{Ru}^{\text{IV}}$		$\text{Ru}^{\text{IV}}/\text{Ru}^{\text{V}}$		$\text{Ru}^{\text{V}}/\text{Ru}^{\text{VI}}$	
	Oxidn	Redn	Oxidn	Redn	Oxidn	Redn
Peaks (mV)	E_{p1a}	E_{p1c}	E_{p2a}	E_{p2c}	E_{p3a}	E_{p3c}
PH 10	-0.074	0.393	0.697	0.320	0.886	0.757
PH 11	-0.531	-0.617	-0.182	-0.207	0.293	0.240
PH 12	-0.103	-0.437	0.540	0.296	0.835	0.765
PH 13	-0.176	-0.439	0.542	0.260	0.816	0.780
PH 14	-0.140	-0.410	0.400	0.381	0.810	0.785

Reaction conditions: *supporting electrolyte: Robinson buffer solutions of different pH's, concentration of the complex (0.001 M). E_{p1a} , E_{p2a} and E_{p3a} are the anodic, while E_{p1c} , E_{p2c} and E_{p3c} are the cathodic cyclic voltammetric peaks potentials respectively, scan rate 100 mVs^{-1} . All data potential in mV vs. FcH/FcH^+ (V). (ferrocene / ferrocenium ion).*

Upon increment of the pH to 11, Figure 3(B) the peaks positions are changed to different potentials as shown in Table 1. Similarly, slight changes in the redox potentials were found at pH = 12 and 13, Figures 3 (C) and (D), this slight change may be due to the formation of a transient $\text{RuO}_2 \cdot n\text{H}_2\text{O}$ on the surface of the electrode.



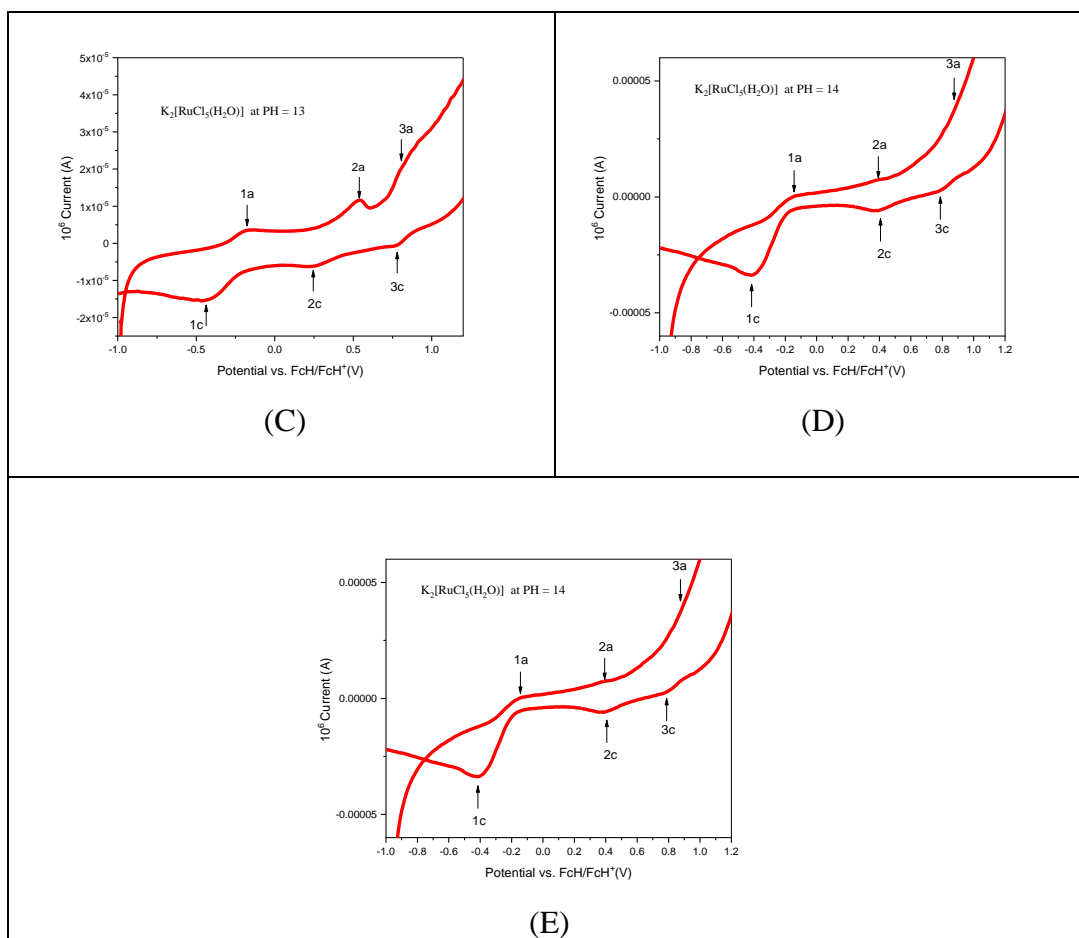


Figure 3. Cyclic voltammograms of $K_2[Ru^{(III)}Cl_5(H_2O)]$: (A) at pH 10, (B) at pH 11, (C) at pH 12, (D) at pH 13, (E) at pH 14, (concentration of the complex (0.003 M), scan rate 100 mV/s).

At pH 14, Figure 3 (E), it was noticed that the oxidation potential increases while the reduction potential decreases, this is probably due to two reasons, the first reason is the high stability ruthenium(VI) ion [40-42] and the second reason is the increment of the pH resulted in deprotonating of the bonded aqua ligand in $K_2[Ru^{(III)}Cl_5(H_2O)]$ complex to form the corresponding stable $K_2[Ru^{(VI)}O_3(OH)_2]$ [44].

3.3. Catalytic hydration of nitriles

The results of the catalytic hydration of nitriles by the catalytic systems $K_2[Ru^{(III)}Cl_5(H_2O)]$ / $K_2S_2O_8$ or NaOCl in a 1.0 M KOH are presented in Tables 2 and 2 (continued).

Benzonitrile was selected as a representative example to optimize the reaction conditions. The complex (5.24 mg, 0.02 mM) is dissolved in 10 mL of 1.0 M KOH, followed by adding of $K_2S_2O_8$, (810 mg, 3 mM) with stirring until the appearance of a red-orange color. Nitrile (2 mM) was then added to that reaction mixture that heated at 80 °C for 4 hrs after which the corresponding amide was

formed, extracted and characterized. A number of factors have been studied to find out the optimum conditions for this catalytic process.

Figure 4a showed that the best amount of the co-oxidant that gave the best yield was found to be 3 mM of $K_2S_2O_8$ (i.e: 150 fold-excess of the catalyst), while with NaOCl lower yields were obtained than that found with $K_2S_2O_8$. This is may be due to that the *in situ* generated $Ru^{(VI)}$ ion is rapidly oxidized to $Ru^{(VII)}$ ion by NaOCl [45]. With $NaBrO_3$ as co-oxidant no amide could be detected and the predominant species is $Ru^{(VII)}$ not $Ru^{(VI)}$ which is not active in this catalytic process. Figure 4b showed the effect of reaction time on the yield of amide, after about 0.75 h there was no amide, this is the induction period through which the active species is formed. It was found that the highest yield of amide was obtained after four hours.

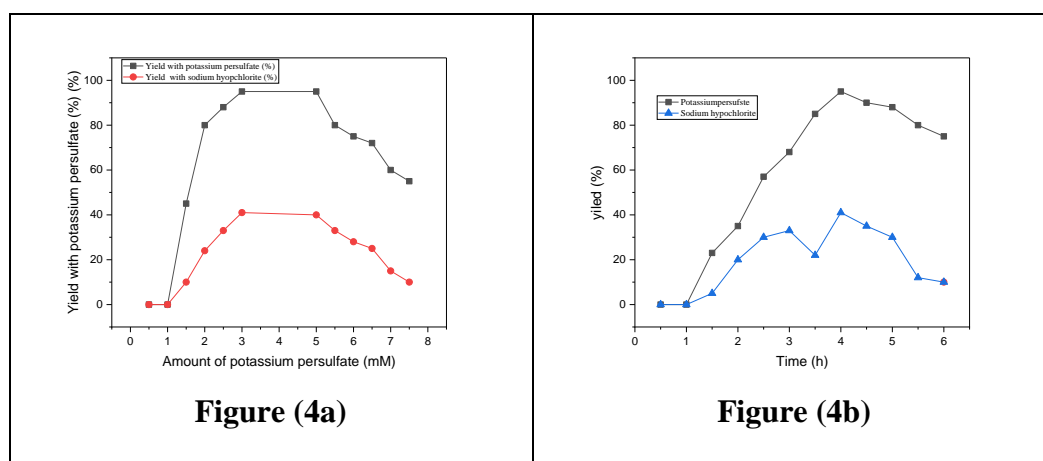
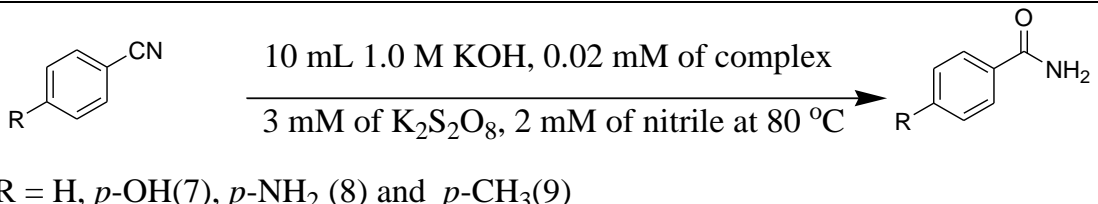


Figure 4a and 4b. The effect of the amount of the co-oxidant (4a) and the effect of the reaction time on the yield (4b).

Attempts were made to find out the amount of the complex that gives the highest yield. All the experimental conditions mentioned above were fixed and three experiments were conducted with three different quantities of the complex, (0.02 mM, Table 2, entry 1^a), (0.03 mM, Table 2, entry 2^a) and (0.05 mM, Table 2, entry 3^a), it was noticed that, increment of the amount of complex more than 0.02 mM did not improve the yield of the corresponding amide. Attempt for hydration of benzonitrile in the absence of the complex (blank experiment) was unsuccessful (Table 2, entry 4^b), since no benzaamide was detected, confirming that the existence of this complex is very essential for this catalytic hydration process. Three experiments were carried out at three different temperatures, 80 °C (Table 3, entry 1^a), 60 °C (Table 2, entry 5^c), and 40 °C (Table 2, entry 6^c), using a thermostated water-bath, we noticed the best yield of benzamide was obtained at 80 °C.

Table 2. Catalytic hydration of nitriles

						
Entry	[Ru ^(III) Cl ₅ H ₂ O] / K ₂ S ₂ O ₈		[Ru ^(III) Cl ₅ H ₂ O] / NaOCl		Reference (32) NH ₃ ·H ₂ O/DMSO/NaOH	Reference (29) RuCl ₂ (PTA) ₄
	Yield (%)	TO	Yield (%)	TO	Yield (%)	Yield (%)
1 ^a	95	190	41	82	93(ref 32)	91
2 ^a	95	190	30	60	-	-
3 ^a	95	190	20	40	-	-
4 ^b	0	0	0	0	-	-
5 ^c	88	176	12	24	-	-
6 ^c	84	168	10	20	-	-
7	95	190	41	82	83	90
8	94	188	33	33	89	-
9	94	168	20	40	81	82

Reaction conditions: Reaction conditions for entries (7, 8, and 9): 10 mL of 1.0 m KOH, 0.02 mM of complex, 3 mM of K₂S₂O₈ and 2 mM of nitrile. Reflux in water-bath for 4 hours at 80 °C. Turn over (TO) = number of moles of product/number of moles of catalyst. ^aRefers to different concentration of complex, ^brefers to the blank experiment, ^crefers to different temperature.

The effect of *p*-substituents was also investigated, yields obtained with *p*-OH, *p*-NH₂, and *p*-CH₃ substituents (Table 2, entries, 7, 8 and 9) are higher than those obtained with *p*-CF₃, *p*-CHO, and *p*-NO₂ Table 2 (continued) entries 10, 11 and 12). This means the electron-donating groups promoted the hydration of *p*-substituted benzonitriles better than the electron-withdrawing groups. Three heterocyclic nitriles, furonitrile, 2-thiophene carbonitrile and 4-pyridine carbonitrile were also hydrated to Furan-2-carboxamide, Thiophene-2-carboxamide and Isonicotinamide in 94%, 92% and 95% yields respectively Table 2 (continued), entries 13, 14 and 15). Upon comparison of our results with some other recent protocols for examples: NH₃·H₂O–DMSO/NaOH [29] and [RuCl₂(PTA)₄] (PTA=1,3,5-triaza-7-phosphaadamantane [32]) It was noticed that our yields are higher see table 2 and 2 (continued) and reaction times are shorter than those reported in these catalytic systems [29,32]. Additionally, the amount of ruthenium catalyst that we used (0.02 mM) is smaller than that reported in [RuCl₂(PTA)₄] system (0.05 mM) [32]. Finally, these reaction conditions are suitable for hydration of these substrates and our protocol is considered to be a greener process since, water is used as a solvent and the reaction is selective and catalytic [46].

Table 2 (continued). Catalytic hydration of nitriles

R = *p*-CF₃ (10), *p*-CHO (11), and *p*-NO₂ (12)

Entry	[Ru ^(III) Cl ₅ H ₂ O] / K ₂ S ₂ O ₈		[Ru ^(III) Cl ₅ H ₂ O] / NaOCl		Reference (32) NH ₃ .H ₂ O/DMSO/NaOH	Reference (29) [RuCl ₂ (PTA) ₄]
	Yield (%)	TO	Yield (%)	TO	Yield (%)	Yield (%)
10	82	164	41	82	-	-
11	84	168	32	62	-	-
12	85	170	25	50	80	89
13	94	188	15	30	-	-
14	92	184	12	24	-	-
15	95	190	20	40	91	-

Reaction conditions: Reaction conditions for entries (10, 11, 12, 13, 14 and 15): 10 mL of 1.0 M KOH, 0.02 mM of complex, 3 mM of K₂S₂O₈ and 2 mM of nitrile. Reflux in water-bath for 4 hours at °C = 80. Turn over (TO) = number of moles of product/number of moles of catalyst.

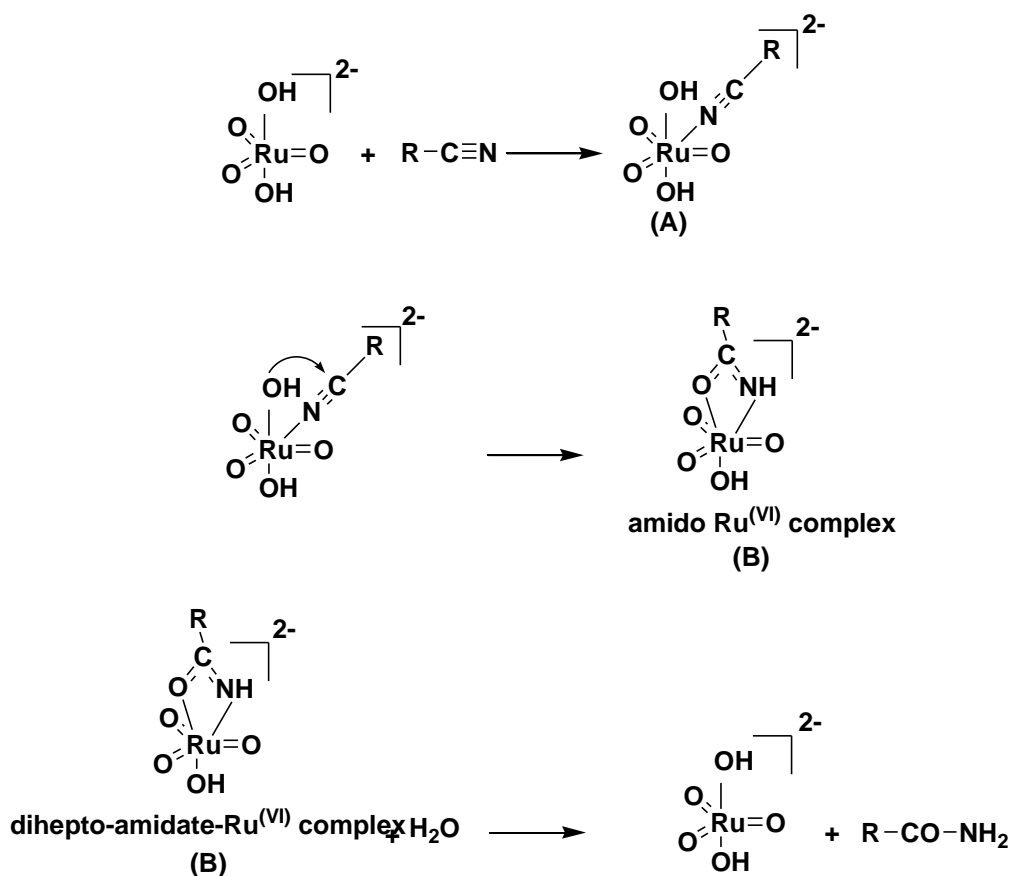
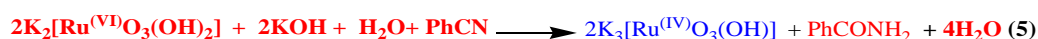
3.4. Recyclability

The aqueous supernatant containing the catalyst was filtered to remove any inorganic solids and evaporated to give a black residue which was washed to remove any salts like K₂SO₄ and KCl. The residue was treated as above in the experimental section and a fresh benzonitrile was added. After 4 hrs the produced amide was extracted and isolated. After the first cycle the yield was 80% and after the second was 60%.

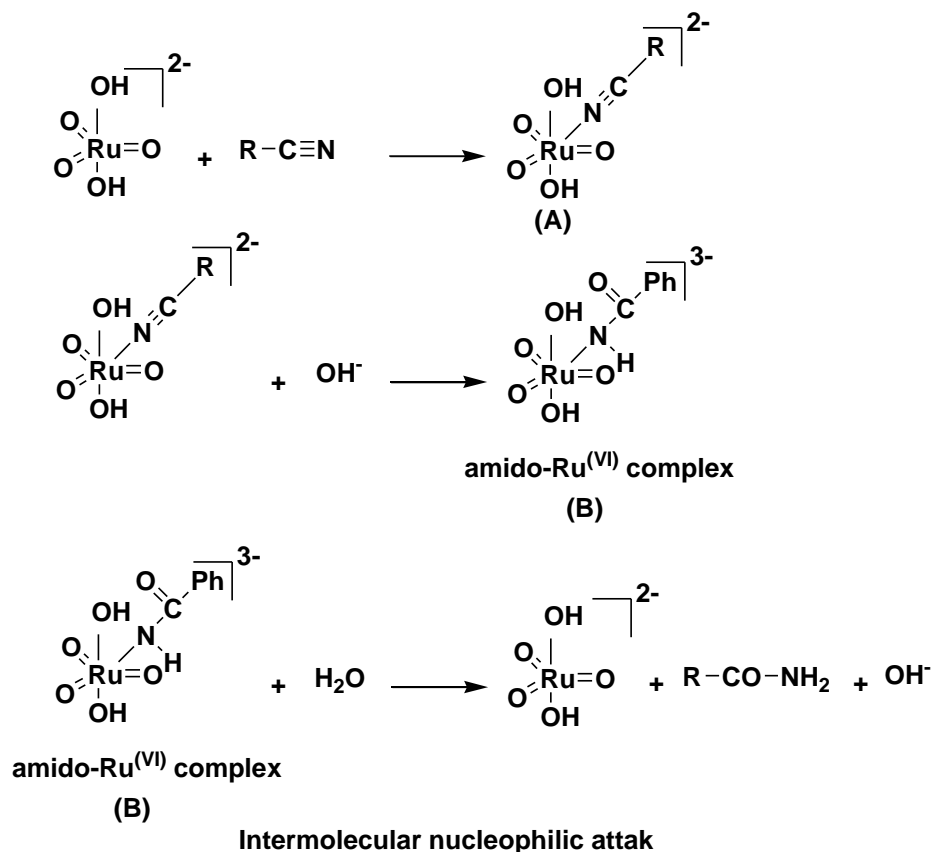
3.5. The proposed mechanism for catalytic hydration of benzonitrile to corresponding amide

The catalytic hydration reactions occur through the formation of the well-known [RuO₃^(VI)(OH)₂]²⁻ anion, [40-42]. The complex K₂[Ru^(III)Cl₅(H₂O)] reacts with an excess of K₂S₂O₈ in an aqueous basic solution, generating the red-orange K₂[Ru^(VI)O₃(OH)₂] solution, (Equation 1) which is stable at (pH 14). The formation of the [Ru^(VI)O₃(OH)₂]²⁻ anion is confirmed by the presence of two bands at 462 nm and 361 nm in the electronic spectrum of the reaction mixture that was used in the catalytic hydration process Figure 2. These bands are close to those reported for the *trans*-[RuO₃^(VI)(OH)₂]²⁻ anion by Griffith [41]. Another evidence, the cyclic voltammogram of complex K₂[Ru^(III)Cl₅(H₂O)] at pH 14 exhibited three redox waves Figure 3. These waves are arisen from the

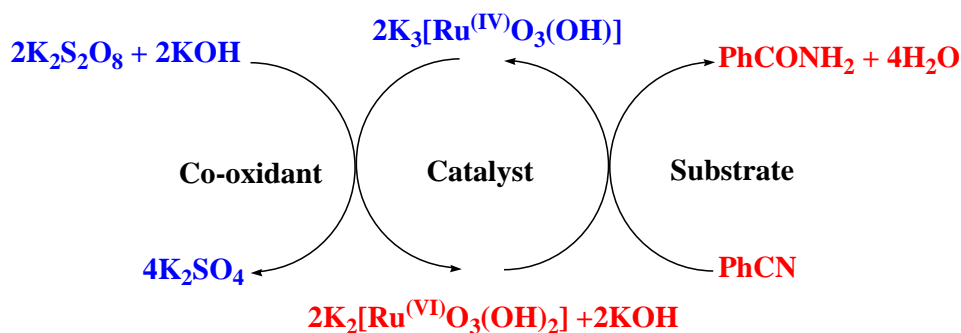
oxidation of Ru(III) to Ru(VI) respectively, as mentioned above in section 3.2. There are two pathways for this mechanism the first one includes coordination of nitrile to $[\text{Ru}^{\text{(VI)}}\text{O}_3(\text{OH})_2]^{2-}$ anion followed by electrophilic attack of the coordinated hydroxyl group on the coordinated cyano group of the nitrile to form the unstable dihepto-amidato complex (B) as intermediate Scheme 1. The complex underwent hydrolysis liberating $[\text{Ru}^{\text{(VI)}}\text{O}_3(\text{OH})_2]^{2-}$ anion and the corresponding amide, this mechanism is called inter-molecular nucleophile attack. The second one involves a nucleophile attack by the hydroxyl group of the aqueous basic medium resulting in the formation of amido-Ru(VI) complex which was hydrolyzed to produce the active catalyst and the corresponding amide Scheme 2. This mechanism is called inter-molecular nucleophile attack. This catalytic cycle Scheme 3, continues until all the substrate consumed as illustrated in equations (5 and 6). Similar mechanism was reported for conversion of nitrile to amide [31]. Attempts are in progress to isolate the amido-Ru(VI) complex.



Scheme 1. Intera-molecular nucleophile attack



Scheme 2. Inter-molecular nucleophile attack



Scheme 3. Catalytic cycle for hydration of nitriles to amides

4. CONCLUSION

The water-soluble pentachloroaquaruthenate(III), $\text{K}_2[\text{Ru}^{(\text{III})}\text{Cl}_5(\text{H}_2\text{O})]$ reacted with an excess of $\text{K}_2\text{S}_2\text{O}_8$ (3mM) or NaOCl (3 mM) but not with NaBrO_3 in a 1.0 M KOH generating the complex $\text{K}_2[\text{Ru}^{(\text{VI})}\text{O}_3(\text{OH})_2]$ *in situ* which catalyzed the hydration of some aromatic and three hetrocyclic nitriles

to their corresponding amides at 80 °C and gave a moderate to high yields. Both spectroscopic and electrochemical techniques confirmed that the active species that generated *in situ* is $[\text{Ru}^{(\text{VI})}\text{O}_3(\text{OH})_2]^{2-}$ ion. The suggested mechanism includes the formation of cyclic amidato complex which is hydrolyzed forming the corresponding amide and the $[\text{Ru}^{(\text{VI})}\text{O}_3(\text{OH})_2]^{2-}$ ion again. This catalytic process continues until all the substrate completely consumed. This protocol can be used in the future for further oxidation of some organic nitriles and also for some functional groups in organic compound.

ACKNOWLEDGEMENTS

The authors would like to thank Taif University Researchers Supporting Project number (TURSP-2020/158), Taif University, Taif, Saudi Arabia, for supporting this work.

References

1. (a) X. Yan, Y. K. Liu, Z. Hao, Z. Han and J. Lin, *Front Chem.*, 7 (2019) 394. (b) A.J.A. Watson, A.C. Maxwell and J.M.J. Williams, *Org. Lett.*, 11(12) (2009) 2667.
2. M. Olivares, P. Knorr, and M. Albrecht, *J. Chem. Soc., Dalton Trans*, 49(6) (2020) 1981.
3. S. Munusamy, P. Muniyappan, and V. Galmari, *J. Coord. Chem.*, 72(11) (2019) 1910.
4. X. Miao, L. Zhang, L. Wu, Z. Hu, L. Shi and S. Zhou, *Nat. Commun.*, 10(1) (2019) 1.
5. D.G. Lee, and L.N. Congson, *Can. J. Chem.*, 68(10) (1990) 1774.
6. Z. Cheng, Y. Xia and Z. Zhou, *Front. Bioeng. Biotechnol.*, 8 (2020) 1.
7. J. E. Bird, C.A. Hammond, K.G. Oberl, K.G. Oberle, E.E. Ramey, Y. Zou, R.C. Lash and C.R. Turlington, *Organometallics*, 39 (21) (2020) 3775.
8. B. Guo, J.G. de Vries and E. Otten, *Chem. Sci.*, 10 (2019) 10647.
9. K-I. Tanaka, S. Yoshifuji and Y. Nitta, *Chem. Pharm. Bull.*, 36(8) (1988) 3125.
10. E.L. Downs D.R. Tyler, *Coord. Chem. Rev.*, 280 (2014) 28.
11. K. Buldurun and M. Özdemir, *J. Mol. Struct.*, 1202 (2020) 127266.
12. M. Al-Noaimi, F.F. Awwadi, A. Hammoudeh, O.S. Abdel-Rahman and M.I. Alwahsh, *J. Mol. Struct.*, 1217 (2020)128327.
13. J.K. Beattie, *Pure and Appl. Chem.*, 62(6) (1990) 1145.
14. T.R. Cundari, and R.S. Drago, *Inorg. Chem.*, 29(19) (1990) 3904.
15. A.J. Bailey, W.P. Griffith, and P.D. Savage, *J. Chem. Soc., Dalton Trans.*, 21(1995) 3537.
16. C. W. Leung, W. Zheng, Z. Zhou, Z. Lin and C. P. Lau, *Organometallics*, 27 (19) (2008) 4957.
17. A.F. Shoair, A.A. El-Bindary, and M.K. Abd El-Kader, *J. Mol. Struct.* 1143 (2017) 100.
18. A.F. Shoair, A.R. El-Shobaky and H.R. Abo Yassin, *J. Mol. Liq.*, 211 (2015) 217.
19. A.F. Shoair and A.A. El-Bindary, *Spectrochim. Acta, Part A*, 131 (2014) 490.
20. C.S. Yi, T.N. Zeczycki and S.V. Lindeman, *Organometallics*, 27(9) (2008) 2030.
21. T-C. Lau and C.-K. Mak, *J. Chem. Soc., Chem. Commun*, 9 (1993) 766.
22. H. Guo, W.-D. Liu, and G. Yin, *Appl. Organomet. Chem.*, 25(11) (2011) 836.
23. W.P. Griffith and M. Suriaatmaja, *Can. J. Chem.*, 79(5) (2001).
24. W.P. Griffith, A.G. Shoair, M. Suriaatmaja, *Syn. Commun.*, 30(17) (2000) 3091.
25. G. Green, W.P. Griffith, D.M. Hollinshead, S.V. Ley and M. Schröder, *J. Chem. Soc., Perkin Trans.*, 1 (1984) 681.
26. A.F. Shoair, A. R. El-Shobaky and E.A. Azab, *J. Mol. Liq.*, 209 (2015) 635.
27. M.S. El-Shahawi and A.F. Shoair, *Spectrochim. Acta, Part A*, 60(1) (2004) 121.
28. R. García-Álvarez, J. Francos, E. Tomás-Mendivil, P. Crochet and V. Cadierno, *J. Organomet. Chem.*, 771 (2014) 93.
29. N. Wang, P. Ma, J. Xie and J. Zhang, *Mol. Diversity*, (2020) 1.

30. T. Mitsudome, Y. Mikami, H. Mori, S. Arita, T. Mizugaki, K. Jitsukawa and K. Kaneda, *Chem. Commun.*, 22 (2009) 3258.
31. M.L. Buil, V. Cadierno, M.A. Esteruelas, J. Gimeno, J. Herrero, S. Izquierdo and E. Oñate, *Organometallics*, 31(19) (2012) 6861
32. W.L. Ounkham, J.A. Weeden, and B.J. Frost, *Chem. Eur. J.*, 25(4) (2019) 10013.
33. E. Manrique, I. Ferrer, C. Lu, X. Fontrodona, M. Rodríguez, and I. Romer, *Inorg. Chem.*, 58(13) (2019) 8460.
34. V.A. Emelyanov, A.V. Virovets and I.A. Baidina, *J. Struct. Chem.*, 49(3) (2008) 566
35. (a) A.F. Shoair, *J. Mol. Liq.*, 206 (2015) 68. (b) Y. Sun, W. Jin and C. Liu, *Molecules* , 24 (2019) 3838.
36. E.E. Mercer and R.R. Buckley, *Inorg. Chem.*, 4(12) (1965) 1692.
37. M.G. Adamson, *J. Chem. Soc. A*, (1968) 1370.
38. C.M. Che, K.Y. Wong and C.K. Poon, *Inorg. Chem.*, 24(12) (1985) 1797.
39. T.C.M. Mak, C.-M. Che and K.-Y. Wong , *J. Chem. Soc. Chem. Commun.*, 1985, 986.
40. A.G.F. Shoair, *Bull. Korean. Chem. Soc.*, 26(10) (2005) 1525.
41. A.J. Bailey, W.P. Griffith, S.I. Mostafa and P.A. Sherwood, *Inorg. Chem.*, 32 (1993) 268.
42. R.E. Connick and C.R. Hurley, *J. Am. Chem. Soc.*, 74 (1952) 5012.
43. T.J. Zerk, P.W. Moore, J.S. Harbort, S. Chow, L. Byrne, G.A. Koutsantonis, J.R. Harmer, M. Martnez, C. Williams and P. Bernhardt, *Chem. Sci.*, 18 (2017) 8435.
44. M. Rodriguez, I. Romero and A. Llobet, *Inorg. Chem.*, 40(17) (2001) 4150.
45. A. Mill and C. Holland, *J. Chem. Res. (S)*, (1997) 368.
46. P.T. Anastas and J.C. Warner, *Green Chemistry Theory and Practice*, Oxford University Press, New York, 1998.

© 2021 The Authors. Published by ESG (www.electrochemsci.org). This article is an open access article distributed under the terms and conditions of the Creative Commons Attribution license (<http://creativecommons.org/licenses/by/4.0/>).